Validity of the Janssen law in narrow granular columns

3 authors:

Ivar Bratberg
Schlumberger Limited
10 PUBLICATIONS **82** CITATIONS

Knut Jørgen Måløy
University of Oslo
243 PUBLICATIONS **6,139** CITATIONS

Alex Hansen
Norwegian University of Science and Technology
405 PUBLICATIONS **9,035** CITATIONS

Some of the authors of this publication are also working on these related projects:

Fiber Bundle Model View project

Immiscible Two-Phase Flow in Porous Media: A Statistical Mechanics Approach View project

Validity of the Janssen law in narrow granular columns

I. Bratberg[1,a], K.J. Måløy[2,b], and A. Hansen[3,c]

[1] Department of Physics, University of Oslo, PO Box 1048 Blindern, 0316 Oslo, Norway and Department of Telecommunications, Norwegian University of Science and Technology, 7491 Trondheim, Norway
[2] Department of Physics, University of Oslo, PO Box 1048 Blindern, 0316 Oslo, Norway
[3] Department of Physics, Norwegian University of Science and Technology, 7491 Trondheim, Norway

Abstract. We have performed experiments on narrow granular columns to test the validity of the Janssen law under such conditions. The weight at the bottom of the cylinder and the compression and movement of the packing have been measured. The apparent mass dependence on height is not in good agreement with the Janssen law using a one-parameter fit. A two-parameter fit yielded good results for the apparent mass during upward and downward movement at constant velocity of the granular column inside the enclosing cylinder. The dependence of the apparent mass on the diameter of the column does not follow the Janssen law. Rather, it depends strongly on details of the packing. A slow force relaxation was observed when stopping the translational stage after upward motion.

1 Introduction

The mechanics of granular materials is an old branch of science [1]. One of its central questions is how one passes from microscopic properties to macroscopic behavior. Many existing macro equations are empiric due to the overwhelming complexity of the underlying microscopic system preventing microscopic derivation of these. One way to connect the macro equations to microscopic properties, is to study their validity for smaller and smaller systems. A systematic study along these lines will provide important clues as to how the macroscopic empiric equations connect to the microscopic level.

One such empiric macroscopic equation is the Janssen law [2,3], stating that the average pressure in granular columns approaches a constant exponentially with depth. This law is more than one hundred years old, and it is still used *e.g.* in silo construction [4,5]. It is difficult to study the Janssen law experimentally as the results are extremely sensitive to the method used to fill the granular column [6]. Even for the same filling method, different results are seen [7]. Vanel *et al.* [8] have reported measurements of the static pressure of a granular pile as a function of the filling height. The ratio between the diameter

of the cylinder and the beads was 10. They found a quite good accordance between the experiment and the Janssen law. However, they introduced a modified version with two parameters to get a better fit. Vanel *et al.* [9] have also checked experimentally different theories for propagation of static forces in a granular cylinder. The Janssen law was checked against the theory of Incipient Failure Everywhere (IFE) [10], and the Oriented Stress Linearity (OSL) model [10]. The conclusion was in favor of the OSL model.

There exists a wide range of theories for the force network in granular media [11]. Of particular interest here is the quasi-elastic model [12] which gives an equation similar to the Janssen law, provided that the defined Poisson ratio of the packing is independent of pressure.

Several experiments and simulations have been carried out on flow of sand in cylinders [13–16]. To model such systems it is necessary to separate the effect of particle friction from the fluid-particle interactions. In the present paper we study particle friction without fluid interaction.

The aim of this paper is to look at the validity of the Janssen law for narrow cylinders. Compared to the experiment of Vanel *et al.* [8] which used a cylinder of diameter 10 bead diameters, the cylinder diameter in our experiments range between 1.9 and 3.5 bead diameters.

In recent work by Bertho *et al.* [17], it is shown that the Janssen law gives a good description of the friction of downward movements. In this paper, we verify this

[a] e-mail: `ivarbra@fys.uio.no`
[b] e-mail: `maloy@fys.uio.no`
[c] e-mail: `Alex.Hansen@phys.ntnu.no`
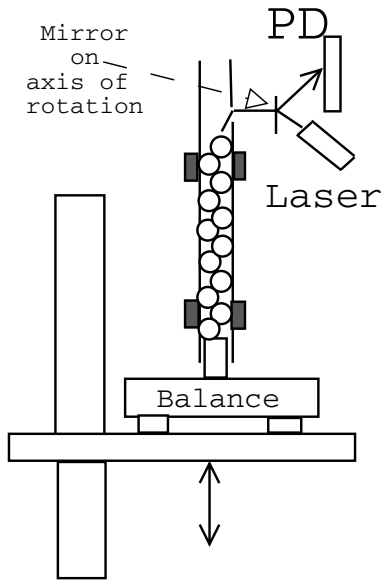
Fig. 1. The experimental set-up consists of a glass column filled with steel balls. The force on the bottom of the packing is measured by a balance. The balance is placed on a vertical translation stage to control the movement of the granular packing. The top level of the granular packing is measured by a laser deflection technique.

rule for very narrow cylinders, and show in addition that the fitting parameters used in the dynamic case correlates strongly with the parameters in the Janssen law. In addition we show that the Janssen law also holds for the case when the packing is translated upward.

In Section 2, the experimental set-up is discussed. In Section 3 the introductory measurements are presented, focusing on the behavior of the systems when moving the bottom plug of the packing in both directions. Section 4 discusses the measurements of the apparent weight as a function of diameter and number of beads.

2 The experimental set up

The experimental set up is illustrated in Figure 1. A boroxid glass tube with an internal diameter d is filled with 20 to 500 steel beads of diameter 3.97 mm and mass 0.256 g. Different tubes of internal diameter 8, 9, 11, 12 and 14 mm where used. The glass tube is fixed in space and kept vertical with a stiff frame. Force measurements are performed by a Sartorius 687 balance, which is placed on a rigid vertical translation stage and the vertical movement is controlled by a DC motor. The velocity used in the experiments was 8.7 μm/s. A brass cylinder is mounted on the balance and placed inside the glass tube from below. The balance, based on strain gages, has a resolution of 0.01 g. The balance acts like an elastic spring with a stiffness constant equal to $k = 1.44$ g/μm $\cdot$ 9.81 m/s^2 = $1.41 \cdot 10^4$ N/m. The stiffness of the translation stage was found to be significantly larger than that of the balance. From the known stiffness of the balance and the well-controlled speed of the translation stage, the position of

the bottom of the packing (or the top of the brass cylinder) was measured.

The displacement of the top of the granular packing was measured by using a laser deflection technique. A hole was made in the glass tube just above the level of the top of the packing. An arm with a fixed rotation axis outside the glass tube went trough the hole and was resting on the highest level of the packing. A mirror was mounted on the rotation axis and a laser beam was reflected from the mirror onto a position sensitive photo-diode. A change in the height of the packing made a rotation of the mirror and a deflection of the laser beam which made it possible to measure the position of the top of the packing with an accuracy better than 2 μm.

The cylinder was filled by dropping one by one bead from 20 cm above the cylinder waiting a sufficient time for each bead to come to rest. By measuring the height of the packing the density was calculated. No significant change in the density was found by changing the specific filling procedure.

3 Qualitative observations of the packing during shear

In order to see how the apparent mass and the density changed during translation the following experiment was carried out: a cylinder was filled with approximately 300 beads. With this amount of beads it is still possible to move the packing upward. The force needed to push the packing upward increases exponentially with the number of beads. The velocity of the translational stage v was chosen as: 1. $v = 8.7$ μm/s for 130 s; 2. $v = 0$ μm/s for 130 s; 3. $v = -8.7$ μm/s for 130 s; 4. $v = 0$ μm/s for 130 s. The positive direction is upward. The velocity was chosen small enough for us to observe the changes and logging it. The time was chosen long enough for the packing to reach a state of stick-slip motion for the upward direction and a stable level for the downward direction. The time between each force measurement was 1.5 s. The measurement cycle, defined by these four points, was repeated many times for the same filling to confirm the repeatability of the experiment. Two of the cycles are presented in Figure 2, represented by solid lines and dashed lines respectively. In the uppermost diagram in Figure 2 the displacement of the translational stage Δy is plotted as function of time. In the next diagram of Figure 2 the weight on the scale normalized with the spring stiffness is plotted as a function of time. Only the changes from the initial values are plotted. Note that the response of the strain gage to a weight Δw gives a change in the bottom position of the granular packing given by $\Delta w/k$. The third diagram from above shows the change of the height Δy_h of the packing, and the bottom curve represents the top level Δy_t of the packing as measured using the laser deflection technique. The figure is split into the four periods by the three vertical lines, each period characterized by the velocity of the translational stage. We see that the form of the curves for the two cycles are similar, but that there
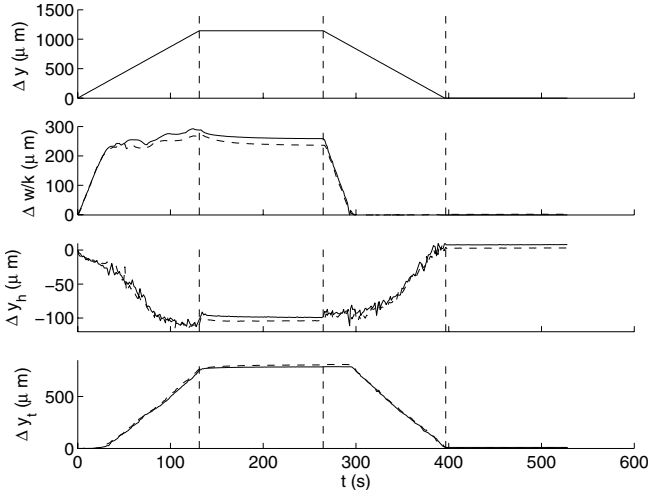
Fig. 2. Two measurement cycles for the same filling are presented, one with solid line the second with a dashed line. From the top: the change of the position of the translational stage, the change of the spring force Δw divided by the spring stiffness k, the change of the height of the packing, Δy_h and the change of the top level Δy_t. The plot is divided in four periods, one for each part of the cycle. Each period is characterized by different velocities of the translation stage. The first period is from 0 to 135 s, the second stops at 270 s and the third at 395 s. The velocities for the periods are 1. $v = 8.7$ μm/s; 2. $v = 0.0$ μm/s; 3. $v = -8.7$ μm/s; 4. $v = 0$ μm/s. The internal diameter of the glass tube for this experiment is 12 mm.

is a certain difference, specially for the upward movement and the relaxation after this. As the movement downward starts, the two curves fall on top of each other.

3.1 The first period

It is natural to divide the first period into three sub-periods. One characteristics of the first sub-period is the monotonic increase in the apparent mass without an increase in the top level Δy_t. In Figure 2 it can be seen that y_t is constant and there is a small compression going on in the first sub-period. To better see when the top starts to move we have magnified the first part of the first period, and separated the three sub-periods with dashed vertical lines see Figure 3. The total height of the packing is decreasing in a short period before the top starts to move. This can be explained by a compactification front in the packing, starting at the bottom and moving upward. As this front reaches the top, the top starts to move, marking the start of the second sub-period in period one. We can see that in the start of the second sub-period, the spring force continues to increase rapidly for a while until it enters a state of irregular stick slip motion, sub-period three. The duration of second sub-period, defined by the period from when the top starts moving until the systems reaches stick-slip state has been observed to increase with the height of the packing. The third sub-period is the region of stick-slip behavior, where the slips appear with negative slopes in the uppermost diagram of Figure 3.
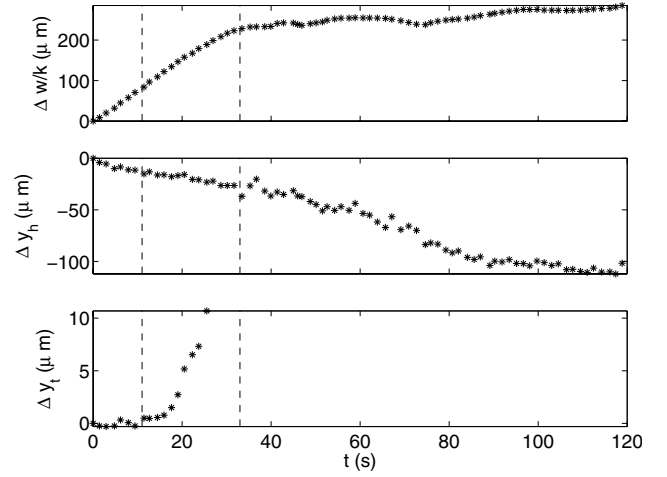

Fig. 3. The first period in Figure 2. The dashed lines separate the three sub-periods in this period. For the upward movement, there is a short period where the packing compactifies, without the top moving. This is the first sub-period. The second sub-period is characterized by a monotonic increase of both the apparent mass and the top level. The third sub-period is characterized by a stick-slip motion. The lower most diagram does not show the whole graph as only the transition from sub-period one to sub-period two is of main interest.
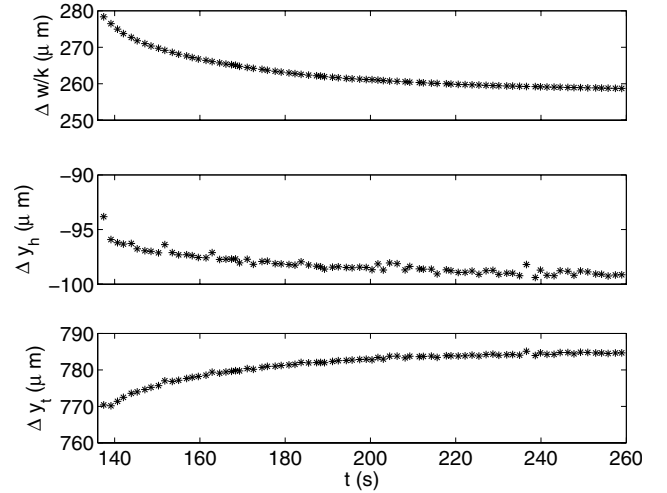
Fig. 4. The relaxation in the second period in Figure 2 we have plotted the change of the spring force Δw divided by the spring stiffness k, the change of height Δy_h and the change of the top level of the packing Δy_t. The packing compactifies with approximately $4\,\mu$m, while the top moves upward approximately $15\,\mu$m.

3.2 The second period

During the second period, the translation stage is at rest after the translation upward. After a fast dilation of about 10 μm, the apparent mass undergoes a slow relaxation. The shear force from the wall on the packing is pointing downward. During the relaxation the global velocity of the packing decreases with time while the top level y_t is increasing. The packing is observed to be compressed around 5 μm during the relaxation, see Figure 4. For this period
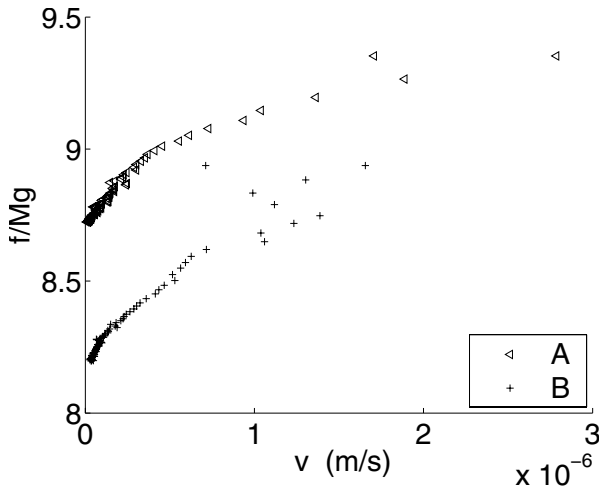
Fig. 5. The global friction normalized with the weight of the beads as a function of the velocity in the second period. The data are calculated from period two in Figure 2. The upper curve with legend A corresponds to the solid curve in Figure 2, while the one with legend B corresponds to dashed curve.

Δy_h is small compared to Δy_t, so the major mechanism is a global movement upward. A similar relaxation have been observed in friction experiments with a single block creeping its way to rest by Berthoud and Baumberger [18]. The observed relaxation was in that case confirmed to be primarily caused by ageing of the static friction force. This type of force relaxation has further been observed in a force measurement of a static granular pile by Løvoll *et al.* due to perturbation by the local force probe [19]. It is important to note that for the case of a granular packing the observed effect may not only be a pure ageing effect but also be influenced by collective effects due to history and velocity dependent internal restructuring of the contact points in the transition from the dynamic regime (period 1) to the static regime (period 2). For the relaxation the global friction force as a function of the velocity is found to increase with the velocity, see Figure 5.

3.3 The third period

The velocity is $v = -8.7$ μm/s. It is natural to divide this period into two sub-periods. The first is characterized by a decrease in the weight at a constant rate with no movement of the top level, and no discernible dilatation. The second sub-period starts when the packing begins to slide against the wall, and the top level starts to move. There is a dilatation during this sub-period. It is interesting to note that upward and downward motion in this experiment are not reversible. In the first period, we found a transient sub-period, defined from the point of where the top starts to move, until the system reaches a state of stick-slip motion. The duration of this transient period was significant in the upward movement, but is hardly seen for downward movement. In the third period, the spring force is constant almost at once the top has started to move.

When the packing is initially at a low density Vanel *et al.* [8] noted a decrease in the density for downward motion. This is in accordance with our observations. In their experiment the apparent mass increased as a function of the descent length. As we observe a significant decrease, this is the opposite of our observations. However it is important to note that the polarization of the friction forces in our experiments when we start the downward motion on average is directed downward because of the upward motion in period 1. This is very different from the experiments by Vanel *et al.* [8] that don't perform upward motion off the granular packing. We therefor expect a decrease in the apparent mass during downward motion in our case due to the change in the polarization of the friction forces.

3.4 The fourth period

The fourth period is a rest period during which the velocity of the translation stage is zero. The variations of forces observed are minimal. Let us compare how the force $\Delta w/k$ relaxes early during the second period with how it relaxes during the fourth period. The second period follows after the packing has been pushed upward, while the fourth period follows after the piston holding the packing has stopped moving downward. We note that there is considerable relaxation in $\Delta w/k$ during the second period while there is very little relaxation during the fourth period, see Figure 2. This may be understood as a result of the contact forces between the grains being larger and there being more contacts during the upward motion than during the downward motion – this again resulting in the change in the direction of the frictional forces with respect to gravity. This increase in contact forces increases plastic flow at the contacts, which in turn leads to larger relaxation. We also note that this scenario is supported by the behavior of Δy_h in Figure 2: in the fourth period, Δy_h is larger than during the second period. Hence, the packing is compactified during the second period in comparison to the fourth period.

4 Quantitative analysis

In this section our results are compared with the Janssen law. It is found that it is not possible to fit the apparent mass as a function of tube diameter as predicted by Janssen, as the properties of the different packing configurations for different fillings play a crucial role. The basic assumptions forming the basis for the Janssen law are:

- The granular material is considered to be a continuum;
- The average stress in the radial direction is proportional with the longitudinal stress:

$$\sigma_{22} = K\sigma_{11}, \qquad (1)$$

where σ is the force per area, 1 is the vertical direction, and 2 the radial direction, K is a positive constant;

- All shear forces from the wall on the beads are at the Coulomb limit and directed in the opposite direction of the imposed velocity. This is a rough assumption, and it is not possible to tell how many of the contacts which are really directed upward and if they are at the Coulomb limit. Even when the friction is not fully mobilized and for a dynamic varying K it may be possible to define an average $\langle \mu K \rangle$. This condition is enough for the equation to fit the data.

Under these assumptions and when the friction force with the wall is directed upward the apparent mass may be written [1,2]

$$M_{\mathrm{app}} = M_\infty \left(1 - e^{-h/\lambda} \right), \qquad (2)$$

where $M_\infty = \pi d^2 \rho c \lambda / 4$, h is the height of the packing, ρ is the mass density of the beads, and c is the solid fraction of beads in the cylinder. Here $\lambda = d\mu K/4$ is the screening length where d is the diameter and μ is the frictional coefficient.

When the packing is mowing upward, the majority of the shear forces from the wall on the packing will be directed downward. In this this case the apparent mass will be

$$M_{\mathrm{app}} = M_\infty \left(e^{h/\lambda} - 1 \right). \qquad (3)$$

The apparent mass corresponds to the granular force which is read by the balance. The height of the packing was found through the relation:

$$\frac{\rho c h \pi d^2}{4} = Nm, \qquad (4)$$

where N is the number of beads, and $m = 0.256$ g is the mass of one bead. It was checked that the solid fraction c was only dependent on the cylinder diameter, and not of the height of the packing. It also did not vary from one filling to another for the same diameter.

In the experiment of Janssen, the apparent mass used in the equation corresponds to the weight measured after transferring the packing downward. We designate this mass as M_{app}^0. It is also interesting to measure the mean value of the weight during downward motion for the period of steady state, M_{app}^-. The mean value of the steady state when the translational stage is moving upward was also measured, M_{app}^+. The corresponding screening lengths we call λ_0, λ_- and λ_+.

First we present some measurements where we change the filling height while keeping the cylinder diameter constant. In Figures 6–8 are shown the apparent mass as a function of the filling height for the three different definitions of apparent mass, M_{app}^0, M_{app}^+ and M_{app}^-. The two sets of data points in each figure correspond to two different fillings. In Figure 8 the direction of the friction force is opposite of that in Figures 6 and 7. The two data sets in each of the three figures separate already for small filling heights. The statistical fluctuations within each data set are much smaller than the separation between the data sets for increasing filling heights. This suggests that the apparent mass depends strongly on the local packing
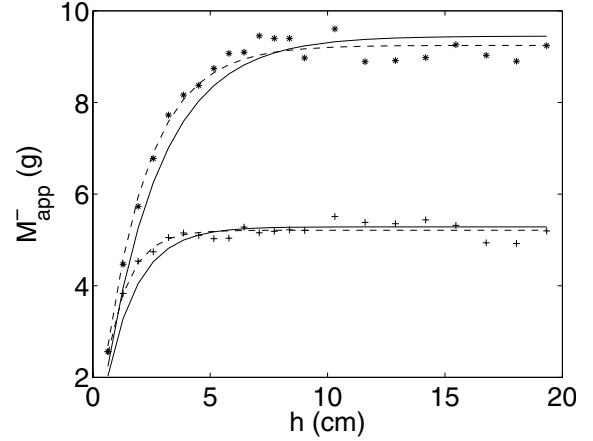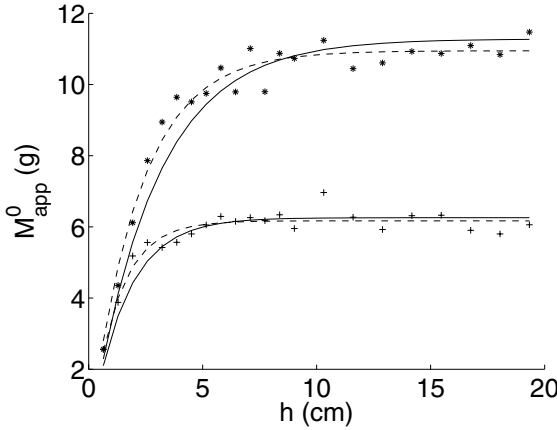

Fig. 6. The apparent mass M_{app}^-, as a function of height, for $d = 11$ mm. The fitted curve is the Janssen law, equation (2). The two different set of data points marked by $+$ and $*$ corresponds to two separate fillings for the same cylinder. The one parameter fits are solid lines, while the two parameter fits are dashed lines. The fitting parameter and the standard deviation for the fitting parameter for the uppermost curve using the one-parameter Janssen law are $\lambda_- = 2.4$ cm and $\delta_{\lambda_-} = 0.039$ cm. For the lower curve the values are $\lambda_- = 1.33$ cm and $\delta_{\lambda_-} = 0.017$ cm. For the two-parameter fits, $\xi = 2.32$ cm, $\gamma = 1.31$ cm for the upper curve, and $\xi = 1.31$ cm and $\gamma = 0.97$ cm for the lower curve.

structure close to the bottom of the column. The solid lines in the figures are the best fit to the Janssen law, equations (2) and (3), with only one fitting parameter λ. The fits contain systematic deviations. The screening length λ appears two places in equation (2) and (3): once in the prefactor (M_{inf}) and once in the exponential. A two parameter equation can be obtained by just take these two instances of λ to be two different constants, ξ in the prefactor and γ in the exponential. The two-parameter fits are plotted as dashed curves in Figures 6–8 and fits well to the experimental data points. This gives an empirical motivation for a two parameter Janssen law. The ratio ξ/γ varies between 1.07 and 2.2 while the average is 1.3 for the different curves. Note that this ratio is expected to change with $K\mu$, as it changes in the simple 2D case, see equations (7) and (8) below.

Here follows a short argument why a one-parameter fit as the Janssen equation not necessarily is the right one for systems where the size of the beads is comparable to the column diameter. It is based on a two-dimensional system. However, the dimensionality does not play an important role here. Consider the two-dimensional packing shown in Figure 9. Assume that a normal force is working upward on the lowermost bead and that the friction force is polarized downward. This correspond to the situation where the packing and the piston is moving upward. A constitutive rule, similar to the one used as a basis for the Janssen equation, is to assume:

$$N_i = KF_i, \qquad (5)$$

Fig. 7. The apparent mass M_{app}^{0}, as a function of height, for $d = 11$ mm. The fitted curve is the Janssen law, equation (2). The two different curves corresponds to two separate fillings for the same cylinder. The one parameter fits are solid lines, while the two parameter fits are dashed lines. The fitting parameter and the standard deviation for the uppermost curve using the one-parameter equation are, $\lambda_0 = 2.8$ cm and $\delta_{\lambda 0} = 0.045$ cm. For the lower curve the values are $\lambda_0 = 1.57$ cm and $\delta_{\lambda 0} = 0.019$ cm. For the two-parameter fits, $\xi = 2.75$ cm and $\gamma = 2.18$ cm for the upper curve, and $\xi = 1.55$ cm and $\gamma = 1.23$ cm for the lower curve.
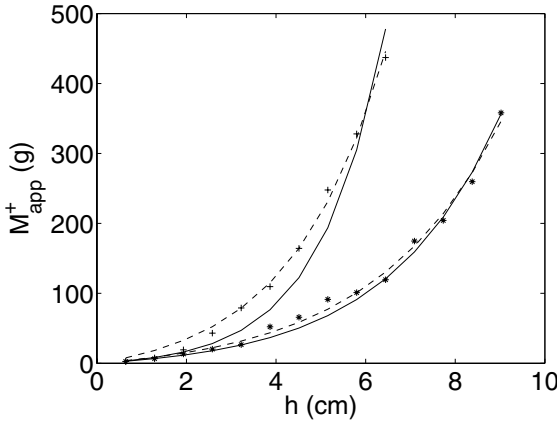
Fig. 8. The apparent mass for upward motion, M_{app}^{+} as a function of height, for $d = 11$ mm. The fitted curve is the Janssen law, equation (2). The two different curves corresponds to two separate fillings for the same cylinder. The one parameter fits are solid lines, while the two parameter fits are dashed lines. The fitting parameter and the standard deviation for the uppermost curve using the one-parameter equation are $\lambda_- = 2.5$ cm and $\delta_{\lambda -} = 0.023$ cm. For the lower curve the values are $\lambda_+ = 1.46$ cm and $\delta_{\lambda +} = 0.014$ cm. For the two-parameter fits, $\xi = 5.44$ cm and $\gamma = 2.1$ cm for the upper curve, and $\xi = 3.77$ cm and $\gamma = 2.83$ cm for the lower curve.

where F_i is the total force in the vertical direction on a center bead, and N_i is the normal forces between the wall and the confined beads just above the center bead. The i is the index of the unit cell, consisting of one center bead and two beads above. It is also assumed that the beads only slide without rotation along the wall. Solving the system for P number of unit cells, gives the following expression
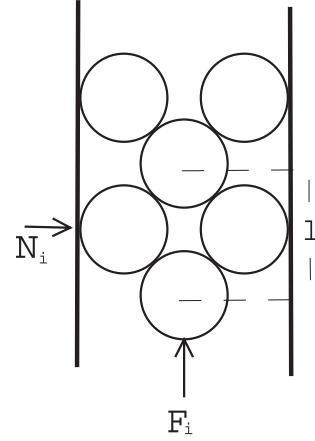
Fig. 9. A two dimensional packing used for the derivation of an alternative to the Janssen equation. l is the height of one unit cell. In the derivation, the particles are supposed to not rotate due to rotational frustration.

for the apparent mass at the bottom:

$$M_{\mathrm{app}} = \xi dc\rho \left(e^{h/\gamma} - 1 \right), \qquad (6)$$

where

$$\xi = \frac{l}{2K\mu}. \qquad (7)$$

Here l is the length of one unit cell, see Figure 9, and d is the width of the column.

$$\gamma = \frac{l}{\log \left(\frac{1}{1-2K\mu} \right)}. \qquad (8)$$

For a typical value of $K\mu = 0.1$ the ratio $\xi/\gamma = 1.12$, and for $K\mu = 0.05$ the ratio is 1.05. For the experiments we do not know the exact equation for ξ and γ. Hence we can explain the systematic deviations seen in Figures 6–8 due to a two parameter dependence. This is confirmed empirically by an excellent fitting of the experimental data with a two parameter fit.

In the following we will use ξ defined as $\xi = 4 \cdot M_\infty/(\pi d^2 \rho c)$ for further analysis as both ξ and γ reflect the same quantity: the degree of force screening. Measurements were done for other diameters as well, and the coefficients ξ_+, ξ_- and ξ_0 (where the subscripts "+", "0" and "–" refer to the motion of the translation stage) were calculated as a function of diameter, see Figure 10. For each filling, a set of ξ_-, ξ_0 and ξ_+ were found. The fluctuations are rather large, and it is not possible to fit the parameters as a function of the cylinder diameter. Fluctuations in γ were found to be of the same order as the fluctuations in ξ and for simplicity we only present the fluctuations in ξ. According to equation (2), $\lambda \propto d$. This is not the case here, and again we argue that this is due to the different packing configurations. This is – as already mentioned – suggested in Figures 6–8, where the two curves in each figure differ much more than the standard deviation of the data points for each curve. The standard deviation of
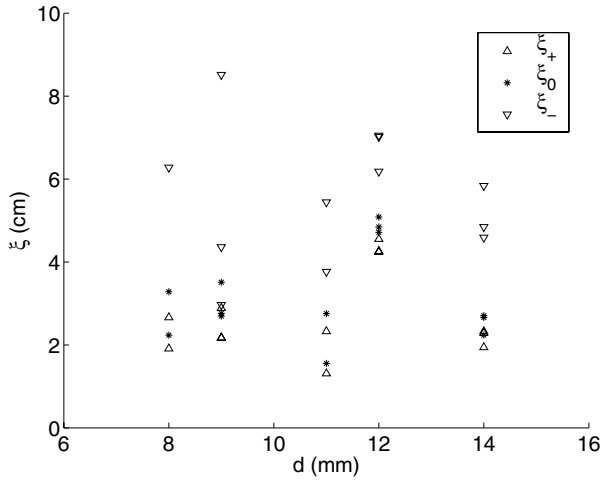
Fig. 10. The fitted parameters ξ_-, ξ_0 and ξ_+ for different diameters. Each symbol represents one filling.

Table 1. The standard deviations of the ξ_- and ξ_0 together with the standard deviations of ξ_f, for downward motion and zero velocity after a downward translation.

Diameter	$\delta_{\xi-}$	$\delta_{\xi0}$	$\delta_{\xi f}$	
	Dyn. down	Static	Dyn. down	Static
12 mm	0.30 mm	0.28 mm	2.6 mm	1.9 mm
14 mm	0.20 mm	0.17 mm	1.9 mm	2.7 mm

the fitting parameters ξ_0, ξ_- and ξ_+ due to the fluctuations of the measuring points around the fits, $\delta_{\xi-}$, $\delta_{\xi0}$ and $\delta_{\xi+}$, were all found to be less that 0.3 mm. In another series of experiments, we filled up the cylinder and measured the apparent mass in the convergence limit, M_∞. We did this ten times for the cylinders of $d = 12$ mm and $d = 14$ mm. From the set of M_∞ values, we calculated ξ_f and the standard deviation $\delta_{\xi f}$. For the 14 mm cylinder we found $\delta_{\xi f} = 1.9$ mm (dyn down), while for the 12 mm cylinder, we found $\delta_{\xi f} = 2.6$ mm (dyn down). The standard deviation taken over different fillings, $\delta_{\xi f}$, are significantly larger than the standard deviations calculated on the basis of the residues of the fittings. This implies yet again that the structure of the packing significantly influences the measured values.

Hence we have given a reason for the large fluctuations, and this is part of the answer on the question: "is the Janssen law valid for small diameters?" We see an exponential dependency of the filling height, as in the Janssen law, but the dependency of the diameter is lost due to the strong influence of the packing structure. Even for the same cylinder we can not expect to get the same parameters for two different fillings. For broader columns the effect of different packings would be expected to average out. We remind the reader that in [8], Vanel *et al.* have performed experiments with the ratio cylinder diameter to bead diameter equal to 10, and no such irregularities were seen. To check the role of frustration we filled a cylinder of 7 mm with beads of diameter 3.97 mm. Each bead inside the cylinder was only in contact with two other beads giving a chain of rotating beads, and no frustration. We could

not observe an exponential decay in this case. This must be due to the lack of frustration. Hence we may propose that frustration is a necessary condition to achieve the exponential dependency of the height which constitutes the essence of the Janssen law.

5 Conclusion

We have studied experimentally granular packings in narrow columns. The apparent mass and the height of the packings have been measured for dynamic as well as static situations. For an upward motion the observations are consistent with a compactification front. The top did not start to move before this front reached the top. After the top started to move, the packing continued to compactify and the apparent mass increased monotonically until reaching a regime of stick-slip behavior.

Creep relaxation was observed in the static regime (regime 2) that may be explained by a combined ageing effect of the friction force, and a collective effect due to internal restructuring of the contact points.

For downward motion the apparent mass decreased almost linearly before reaching a steady state and the top started to move. After the top had started to move for the downward motion, a dilation was observed in the packing.

Even for very small diameters, the apparent mass has an exponential decay. But the Janssen law does not fit satisfactory with a one parameter fit, and we argue for a two-parameter fit for small systems. The necessary condition for a exponential decay is shown to be rotational frustration and that the frictional forces are directed due to translation of the packing. The exponential decay is not observed for a column so narrow that each bead has only two neighbors. The two parameter Janssen law is observed to hold for the static case, which is the common setting. It also holds for upward movement and downward movement as well. For the narrow cylinders as was used in this experiment, it is not possible to fit the Janssen law dependence on the diameter. The packing structure is the dominant factor for such small diameters.

References

1. J. Duran (ed.), *Sands, powders and grains: An introduction to granular materials* (Springer Verlag, Berlin, 1999)
2. H.A. Janssen, Z. Verein Deutsch. Ing. **39**, 1045 (1895)
3. R.M. Neddermann, *Statics and kinematics of granular materials* (Cambridge University Press, Cambridge, 1992)
4. C.V. Schwab, I.J. Ross, G.M. White, D.G. Colliver, Trans. ASAE **37**, 1613 (1994)
5. S.A. Thompson, N. Galili, R.A. Williams, Trans. ASAE **39**, 1093 (1996)

6. T. Jotaki, R. Moriyama, J. Soc. Powder Technol. Jpn. **14**, 609 (1977)

7. J.H. Shaxby, J.C. Evans, Phil. Trans. Faraday Soc. **19**, 60 (1923)

8. L. Vanel, E. Clement, Eur. Phys. J. B **11**, 525 (1999)

9. L. Vanel, P. Claudin, J.P. Bouchaud, M.E. Cates, E. Clement, J.P. Wittmer, Phys. Rev. Lett. **84**, 1439 (2000)

10. J.P. Wittmer, P. Claudin, M.E. Cates, J.P. Bouchaud, Nature **382**, 336 (1996)

11. P.G. de Gennes, Rev. Mod. Phys. **71**, 374 (1999)

12. P. Evesque, P.G. de Gennes, C. R. Acad. Sci. (Paris), Ser. II **326**, 761 (1988)

13. E.G. Flekkøy, S. McNamara, K.J. Måløy, D. Gendron, Phys. Rev. Lett. **87**, 134302 (2001)

14. D. Gidaspau, *Multiphase Flow and Fluidization* (Academic Press, San Diego, 1994)

15. J.L. Aider, N. Sommier, T. Raafat, J.P. Hulin, Phys. Rev. E **59**, 778 (1999)

16. T. Raafat, J.P. Hulin, H.J. Herrmann, Phys. Rev. E **53**, 4345 (1996)

17. Y. Bertho, F. Giorgiutti-Dauphine, J.P. Hulin, Phys. Rev. Lett. **90**, 144301 (2003)

18. T. Baumberger, Europhys. Lett. **41**, 617 (1998) and T. Baumberger, L. Gauthier. J. Phys. France I **6**, 1021 (1996)

19. G. Løvoll, K.J. Måløy, E.G. Flekkøy, Phys. Rev. E **60**, 5872 (1999)